Bull. Fac. Fish. Hokkaido Univ.
37(3), 190-206. 1986.

Hydrodynamic Characteristics in Simplified Components of Artificial Reef Structures

Cheng-Hai WANG* and Osamu SATO*

Abstract

A series of representative models, such as the cylinder, triangular prism, quadrangular prism and square prism, were chosen for this experiment after considering the various components of artificial reef structures in current use. Through flow visualization and a newly designed strain gage sensor, the basic hydrodynamic characteristics of the eddy generated by models were qualitatively observed and quantitatively examined separately in a small-scale water tank and a large-scale water channel. Those parameters associated with the eddy were analyzed by computer. The following results were obtained: two variations of eddy attenuation were observed in the eddy area for each model - the first was characterized by strong fluctuations and the second by gentler ones, but the frequency of the eddy was an unchangeable parameter; the Strouhal number was different for each model and was in inverse proportion to the drag coefficient of the model; the weaker the variation in eddy strength, the higher the frequency and, conversely, a stronger variation in eddy strength accompanied a lower frequency; the distance and width of the effective eddy range were influenced by models and corresponded with the frequency of eddy and eddy strength. In short, each model had distinguishable hydrodynamic characteristics and parameters related to the eddy were all interrelated variables. Experimental results indicate that optimal artificial reef structures which have specific functions for certain species can be constructed by basing the design of artificial reef structure on the distinguishable hydrodynamic characteristics of each structural components.

Introduction

Research on artificial reefs has been conducted for several decades in Japan, America, China and other areas of the world (Ohshima, 1954; Sato, 1984; D'Itri, 1985; Bohnsack et al., 1985; Chang, 1985; Pollard et al., 1985). In general, reefs effectively attract and aggregate fishes and other organisms (Ogawa, Y. 1968), but artificial reef structures have some different characteristics from natural reefs. Some of the species that gather at artificial reefs are more abundant in terms of density than those same species gathering at natural reefs, however, the kinds of species that aggregate on natural reefs are more diverse than those species aggregating on artificial reefs (Burchmore et al., 1985; Matthews, 1985; Hori, 1985). In terms of attracting fish, artificial reef structures can be made more effective than the natural reefs (Sonu, 1981; Resource Association of Japan, 1985; Jessee et al., 1985). It has been reported that some structures are very effective while some structures are ineffectual (Nakahara, 1982; Yamane, 1984; Feigenbaum et al., 1985).

* *Laboratory of Fishing Gear Engineering, Faculty of Fisheries, Hokkaido University, Hakodata, Hokkaido, 041 Japan*
(北海道大学水産学部漁具設計学講座)

At present, structural units are usually randomly dumped onto the seabed resulting in a large-scale "trial and error" experiment, as the construction and placement of these reefs are not based on proper scientific principles and whether or not they will be effective is simply a kind of "random hope". Based on the accumulated data concerning artificial and natural reefs, it appears that the structure of artificial reefs may play an important role in attracting fish, i.e., different types of reef structures may have distinguishable hydrodynamic characteristics in the moving waters, such as frequency properties of the eddy, changes in strength of vortices, and effective ranges. In other words, the structural design should be based upon exact scientific data and scientific principles to optimize effectiveness. However, studies on hydrodynamic aspects are still insufficient and only a few papers have dealt with those factors to date (Sato, 1977 ; Sakuda, 1980).

In this experiment, variously shaped components of current artificial reefs were considered and a series of representative models were chosen for analyzing the basic hydrodynamic characteristics of them to determine the mechanism of the variables associated with the eddy generated by models. Further, it was attempted from a hydrodynamic point of view to explain the phenomena occurring on artificial reefs and to offer suggestions for the design of optimal structures in the future.

As for the vortices generated by an object, many fundamental studies, both theoretical and experimental, have been made in the field of Fluid Mechanics, also known as "Karman Vortex", however, much of this research was limited in scope and results do not directly relate to the design of artificial reefs (Kanamoto, 1959 ; Adachi et al., 1983 ; Noto, et al., 1983 ; Igarashi, 1984). Through the flow visualization based on these studies, flow patterns with different models and similar models of different sizes were observed and qualitatively analyzed. A new type of strain gage sensor was designed for measuring the variables associated with the eddy and the algorithm of FFT (Fast Fourier Transform) was utilized in the program for quantitative analysis. The frequency properties of the eddy, variations in eddy strength and effective range of the eddy behind models were quantitatively examined. Results of qualitative and quantitative analyses showed that the different models can be distinguished by different hydrodynamic characteristics.

Materials and Methods

A series of five models were chosen as the simplified components for artificial reef structures and the flow direction is indicated by the arrow as shown in Fig. 1. There were five different sizes for each model with a maximum projected width of 20, 40, 60, 80, 100 mm and a length of 300 mm ; in total, there were 25 kinds of models used in this experiment. All models, except cylinders, were made of 5 mm thick vinyl chloride sheet, an organic adhesive agent (**TAKIBOND** No. 200) was used for bonding the parts and sandpaper was used for polishing the surfaces. Cylinders made of acrylic resin were purchased. During the experiment, models were arranged according to the changes in degree of angle in the order of cylinder (Model 1), triangular prism 1 (Model, 2), quadrangular prism (Model 3), triangular prism 2 (Model 4), and square prism (Model 5).

In an attempt to visualize the eddy generated by an object, analyze flow patterns and improve the methods for quantitative ananlysis, a small-scale contra-

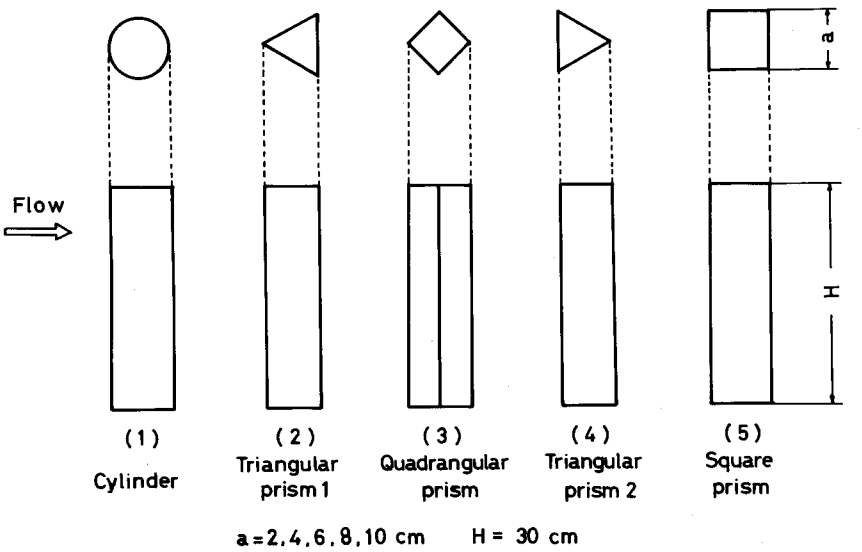

Fig. 1. Simplified models of components for artificial reefs used in this experiment.

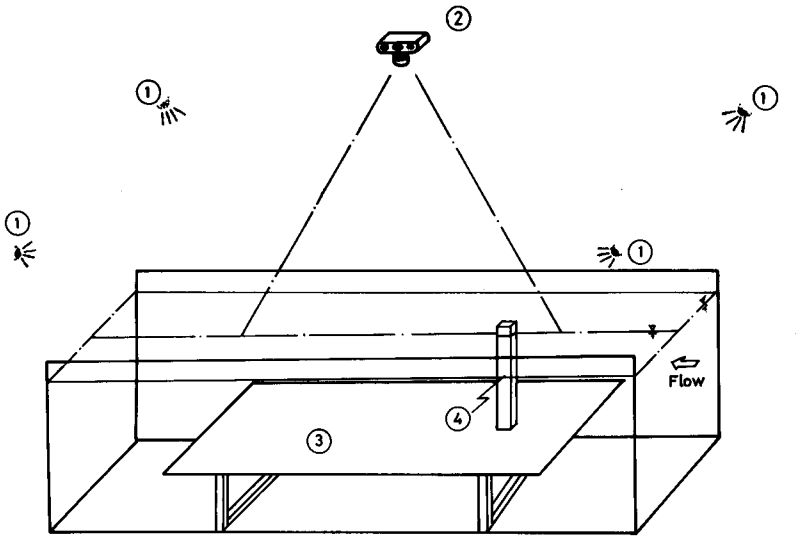

Fig. 2. Apparatus arrangement for flow visualization.
1 : lamp 2 : camera 3 : black plate 4 : model

circulating water tank was used for flow visulization. Main dimensions of the tank were $1200 \times 1200 \times 500$ mm and an impeller powered by a motor was used to circulate the water. The imbalance of the flow speed caused by the impeller was rectified by guide vanes placed in the tank. For photograghs, a Nikon-F2 camera was used with four lamps (500 W, 100 V) installed at four points. A sketch of the equipment for flow visualization is shown in Fig. 2. Models were fixed to the black plate with

screws at bottom.

There are many methods for flow visualization (Asanuma, 1979). In this experiment, the Tracer-Suspension method was utilized and aluminum powder was used as a tracer. It was reported that for this method, the most suitable speeds are from 5 cm/sec to 30 cm/sec with 50 cm/sec being the limit because of the existing effects of gravity and surface tension of water. Accordingly, a flow speed of 20 cm/sec was chosen for the flow visualization. The shutter speed of the camera was set at 1/15 sec to photograph the streamlines of flow resulting in a series of photos of visible flow patterns. The information obtained regarding hydrodynamic characteristics, however, was limited and incomplete, so further quantitative experimentation was necessary.

Based on these previous qualitative experiments, further quantitative experiments were conducted. Those parameters related to the eddy which were generated by models were measured and analyzed (Fig. 3). Using a current meter for detecting the frequency of the vortices behind a model posed problems because, in the eddy area, the current direction varied quite frequently and the presence of bubbles considerably effected the precision of the current meter. Even if accurate measurements of velocity changes in the eddy area could be obtained, pressure changes would also be difficult to calculate since pressure changes in the eddy may not be in proportion to the square of the velocity and, as a result, any further analyses would be limited. In order to avoid these problems and more conveniently measure the physical parameters, a strain gage sensor was designed for this purpose (Fig. 4). It consisted of four strain gages, a steel body with bars and plates, and a bridge circuit was utilized. The sensor was made sensitive to any small changes in the current under the experimental conditions. The response of the sensor was tested with weights, and was found to be balanced on both sides. The natural frequency of the free vibration was 26 Hz and it was found that the sensor had almost no effect on the eddy. The strain amplifier (DS6/MDC, SHINKOH) was connected to the sensor and through the amplifier the value of the original changing voltage, which was fed into the computer for further calculations and analyses, was obtained.

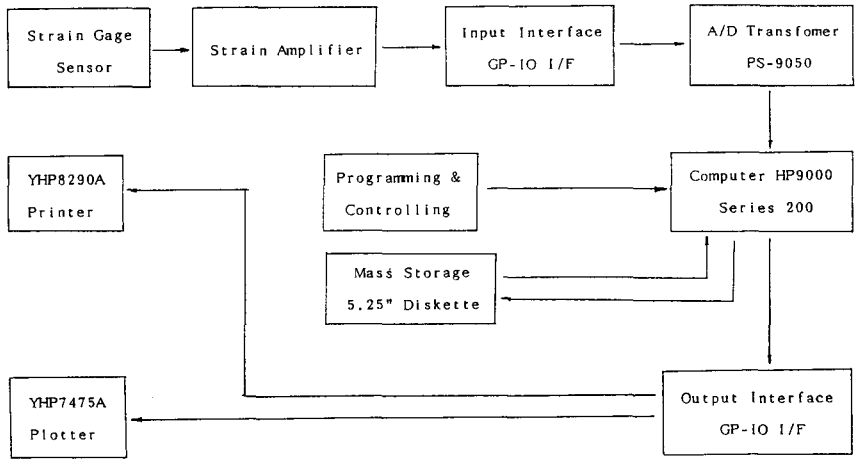

Fig. 3. Block diagram of measuring system for quantitative analysis.

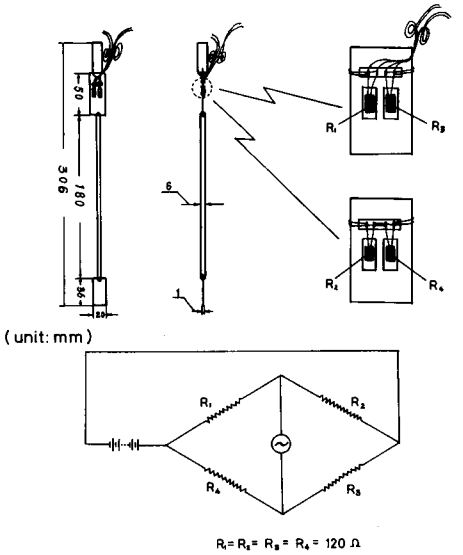

Fig. 4. Strain gage sensor for measuring eddy strength and detecting frequency.

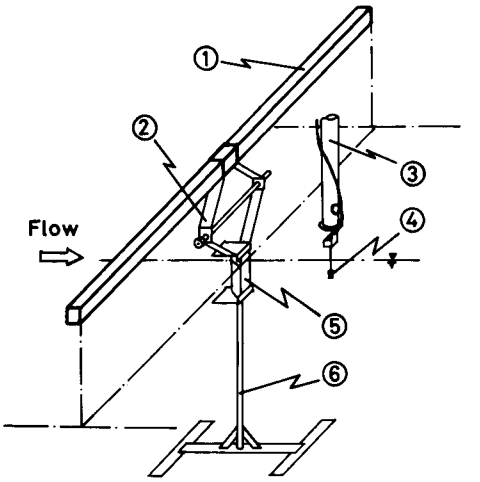

Fig. 5. Sketch of equipment for setting models.
1 : cross beam 2 : jack
3 : traverser 4 : sensor
5 : model

A large-scale horizontal type water channel was utilized for the quantitative anlysis. The main dimensions of the channel were $24.8\times10\times1.2$ m with the test section being $6\times2\times1$ m. A 22 KW motor in the channel system powered two paddle wheels and generated the flow in two side channels. With the guide vanes in place, a uniform flow could be obtained in the central water channel. The relation between the flow speed and the voltage for powering the motor can be expressed as $V=0.0505U+0.727$, where V is voltage and U is flow speed. Using this formula, the programs were written and the flow speed was conveniently controlled through computer. Equipment, which was designed to set models in the water channel, consisted of a stand and a cross beam with an attached jack (Fig. 5). The stand was used to support the models, the cross beam was fixed at two side walls of the central water channel and the jack was attached to the central part of the beam. Thus, the models could be firmly fixed between the jack and stand for measuring.

Several non-dimensional parameters were used to decide the measuring points : the parameter a expressed the maximum projected width of models ; A, the distance from the back of the model to any given measuring point along the central line of the model ; B, the perpendicular distance from any measuring point to the central line. Using the non-dimensional parameters A/a and B/a, any point could be accuratly expressed and the hydrodynamic characteristics of different models in the eddy area could be compared. A three-dimensional traverser was used to move the sensor. It had a moving range of $2000\times1000\times1000$ mm allowing the sensor to be moved precisely to any given measuring points.

Through dimensional analysis, it was found that the parameter f(frequency of the eddy generated by models) was highly influenced by the variables U(velocity),

D (dimension of model), and ν (kinematic viscosity). The equation g (U, D, ν, f)=0 can be used for each kind of model. Utilizing the π theorem, the two non-dimensional parameters, $\Pi_1 = f \cdot D/U$ and $\Pi_2 = U \cdot D/\nu$, can be represented, as a result, the relationship can be expressed as : $f = U/D \times h(U \cdot D/\nu)$. In this experiment, the parameter ν was a constant and it was only necessary to consider the parameter f with the parameters U and D in terms of frequency properties.

To measure the variations in the eddy strength and compare the hydrodynamic characteristics with different or similar models, the maximum value of the pressure perpendicular to the flow direction in analog data was taken as a representative parameter P and the pressure coefficient was defined as $CP_x = P/(0.5 \cdot \rho \cdot U^2)$, U(velocity), ρ (density of water).

For calculating the frequency from analog data obtained by the strain gage sensor, the algorithm of FFT (Fast Fourier Transform) was written into the program. Much has been written concerning the optimal conditions of calculation for this algorithm (Yoshizawa, 1969 ; Yonezawa, 1972 ; Takahashi, 1973 ; Hino, 1977). In this experiment, 256 data points were chosen, the sampling frequency was 10 or 20 Hz, and the sampling time was 25.6 or 12.8 seconds for the stability of the analog data. Since the maximum frequency of the vortices was lower than 5 Hz, the aliasing phenomenon was avoided, i.e., $\Delta t < 1/(2f_c)$, where f_c is the maximum frequency in phenomenon when using the FFT.

The energy distribution with frequencies became clear through power spectra. Through further use of the analysis programs for data, the eddy strength and power spectra of different models, velocities, and different measuring points in the eddy area were compared and the basic hydrodynamic characteristics of vortices were clearly discernible.

Results

Flow patterns

Flow patterns of similar and different models were obtained through the flow visualization (Fig. 6). It was discovered that different models with the same maximum projected width had different flow patterns both in terms of width of the eddy area and pitch between vortices. The cylinders had the biggest pitch between vortices, and their observed speed was relatively fast, however, the width of the eddy area was the narrowest of all models. In comparison, the square prisms had the smallest pitch between vortices and their observed speed was relatively slow, but had the greates width in terms of eddy area. It was also observed that similar models had similar flow patterns. When five different sizes (20, 40, 60, 80 and 100 mm) were compared for each model, the pitch between vortices and width of vortices were similar but the eddy area became larger as the size of the model increased and the frequency of vortices decreased.

Further, two types of vortices were observed for the square prisms. Before the main vortices were generated, smaller vortices had first attached to the sides of the models and then moved away from the sides to join the main vortices.

Frequency properties of the eddy

The relation between the dominant frequency and the flow speed was obtained

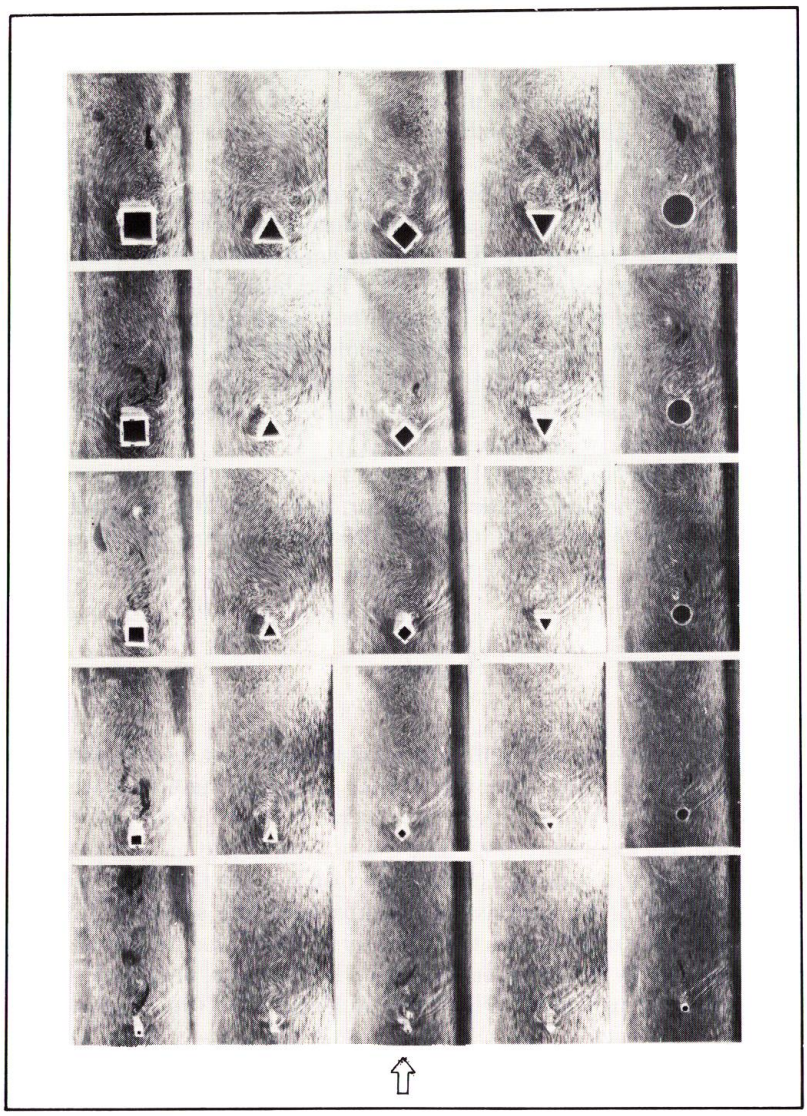

Fig. 6. Flow patterns with similar and different models in projected width of 20, 40, 60, 80 and 100 mm and arrow indicating flow direction.

for each model. The disturbance levels compared with each dominant frequency at different speeds are shown in Fig. 7 ; Fig. 8 shows the results for different models with different frequencies. As the flow speed became greater than 15 cm/sec, the cylinder had the highest frequency and the square prism had the lowest frequency of all models, which corresponded with observations of flow visualization.

Since the Strouhal number is a function of the Reynolds number and is a representative non-dimensional parameter for describing the characteristics of vor-

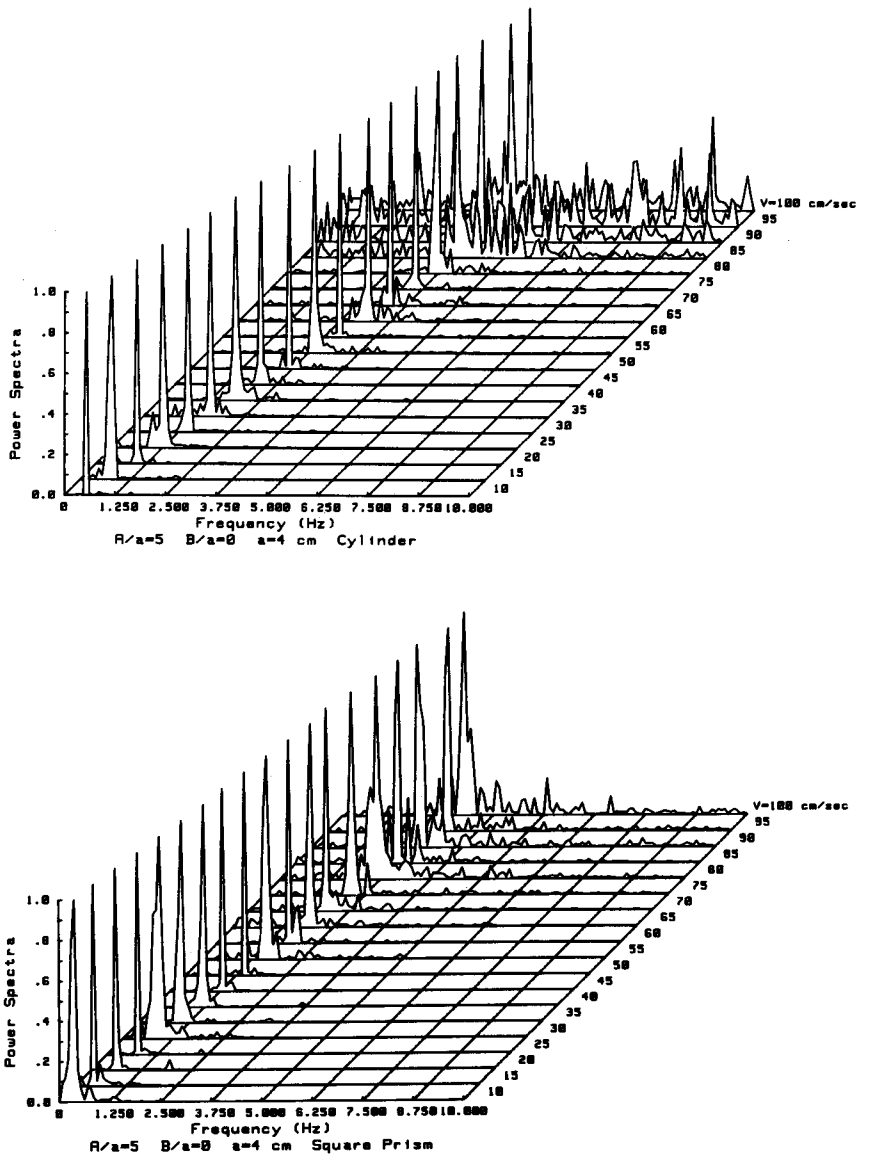

Fig. 7. Power spectra in relation to various velocities with relative disturbance levels.

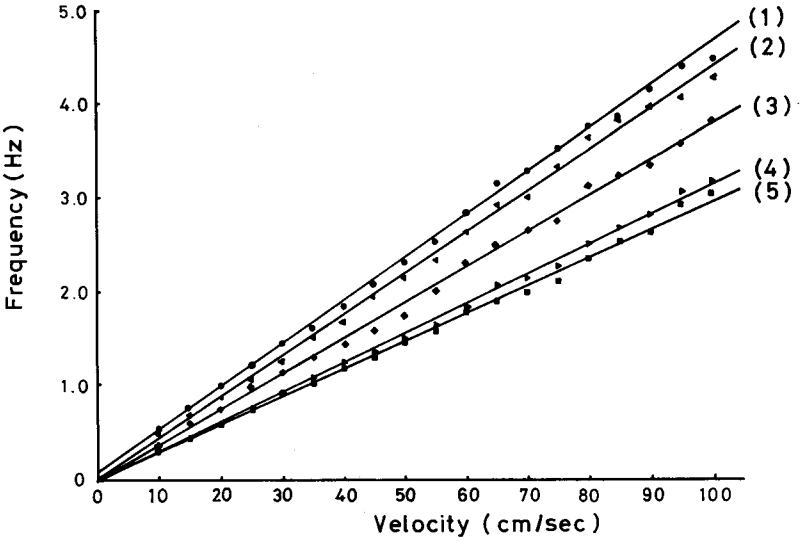

Fig. 8. Relations between dominant frequency and velocity with different models in same projected width of 40 mm.

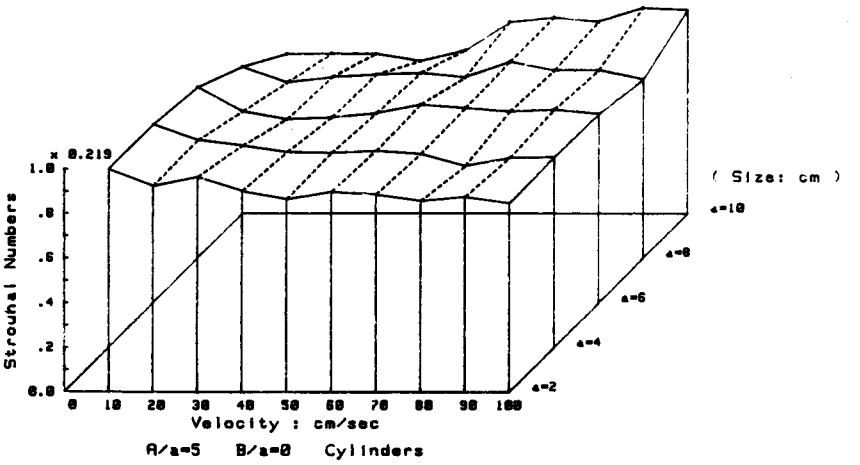

Fig. 9. Relations between the Strouhal number and velocity with different sizes for cylinder.

tices generated by an object, the relation between both is shown in Fig. 9. Because ν (kinematic viscosity) was a constant in this experimental condition of 19-20°C and the Strouhal number varied only according to the flow speed and the model size, this three-dimensional representation shows that the Strouhal number had almost no change in relation to the Reynolds number. Further, when the Strouhal number was compared with the drag coefficient, it was discovered that they were correspondent (Table 1).

Table 1. The Strouhal number of different models compared with drag coeffient

	Cylinder	Triangular Prism 1	Quadrangular Prism	Triangular Prism 2	Square Prism
Strouhal Number	0.19	0.18	0.15	0.13	0.12
Drag coefficient	1.2	1.6*	1.6	2.0*	2.1

* right-angled triangle (Re : $2.0\times10^3\sim9.9\times10^4$)

Eddy strength with velocities

As velocity increased, the pressure perpendicular to the flow direction also increased, as shown in Fig. 10. The function $P=k\cdot U^b$, where P is pressure, U is velocity, and k and b are coefficients for comparing the eddy strength, was used to express variations in eddy strength at different velocities. With the median value of coefficient $b(\bar{b}=1.74)$, the value of coefficient $\bar{k}$ was obtained for each model (Table 2). Results showed that variations in eddy strength were in inverse proportion to the changes in the frequency of vortices and were not in proportion to the velocity squared. It was shown that the parameters of the eddy were interrelated.

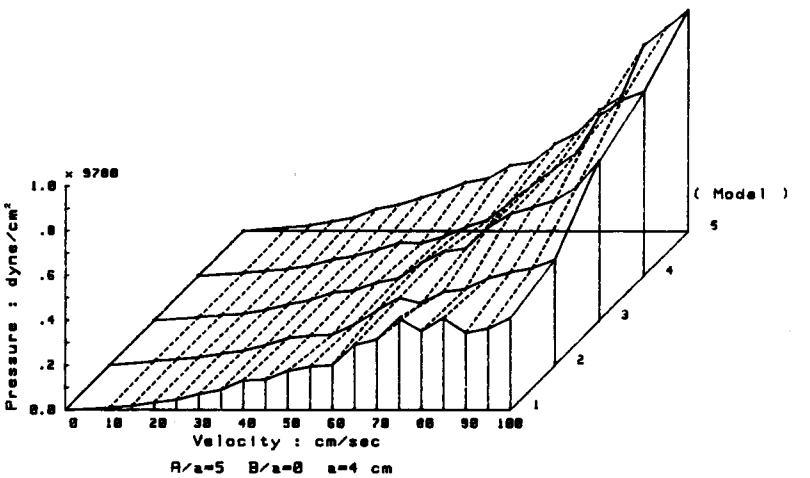

Fig. 10. Relations between pressure and velocity with different models.

Table 2. Values of a and b in formula $P=aU^b$ and value of a calculated using median value b

$P=kU^b$	Cylinder	Triangular Prism 1	Quadrangular Prism	Triangular Prism 2	Square Prism
b	1.64	1.54	1.81	1.90	1.78
k	2.53	3.75	1.50	1.60	2.54
$\bar{b}$	1.74	1.74	1.74	1.74	1.74
$\bar{k}$	1.76	1.81	1.96	2.20	2.56

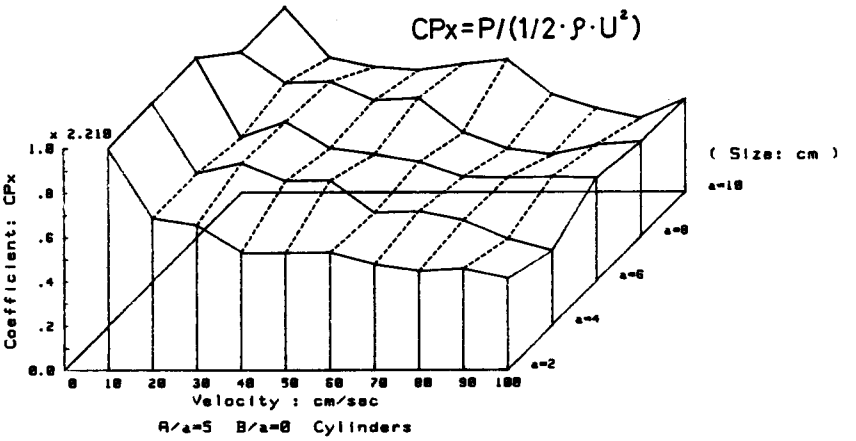

Fig. 11. Relations between pressure coefficient and velocity with different sizes for cylinder.

Table 3. Values of c and d in formula $CPx=cU^d$ and value of c calculated using median value d

CPx=cUd 2	Size (cm)				
	4	6	8	10	
d	−0.35	−0.40	−0.32	−0.35	−0.32
c	4.66	5.90	4.34	4.46	3.88
d	−0.35	−0.35	−0.35	−0.35	−0.35
c	4.65	4.80	4.84	4.47	4.27

The pressure coefficient CP_x was used to compare the eddy strength with similar models of different sizes, results are shown in Fig. 11. The function $CP_x=c\cdot U^d$ was used to express the variation of the CP_x, where c and d are coefficients. Further, with the median value of the coefficient $d(\bar{d}=-0.35)$, the coefficient $\bar{c}$ was obtained for each model (Table 3). It was found that the CP_x decreased as velocity increased since $CP_x=P/(0.5\cdot\rho\cdot U^2)$. The variation in pressure was not in proportion to the square of the velocity, eddy strength was nearly unchangeable with different sizes for similar models, and hydrodynamic characteristics were geometrically similar in terms of eddy area, in the case of the point $A/a=5$, $B/a=0$. For cylinders, the relation between the pressure and the velocity can be expressed as $P=2.30U^{1.65}$ from $CP_x=4.61\cdot U^{-0.35}$.

Effective range of the eddy

The variables related to the vortices were measured at a series of points. It was observed that the vortices generated by models first developed and were then attenuated at a certain point in the flow. This process of development and attenuation was similar among the eddies generated by different models, but the points at which the peak value appeared were different as were the peak values themselves, with the peak point shifting toward the upstream direction from $A/a=4$ to $A/a=$

2 (Fig. 12). The power spectra, i.e., energy distribution with frequencies in the eddy area, were analyzed for each model (Fig. 13). From these results it was discovered that the frequency of the eddy was unchanged in the eddy area and that there were two variations in terms of energy attenuation : the first being character-

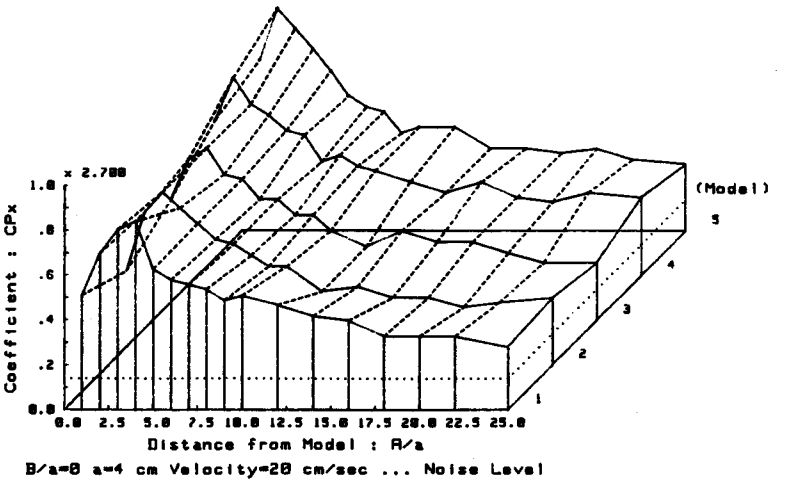

Fig. 12. Changes of pressure coefficient in back eddy area.

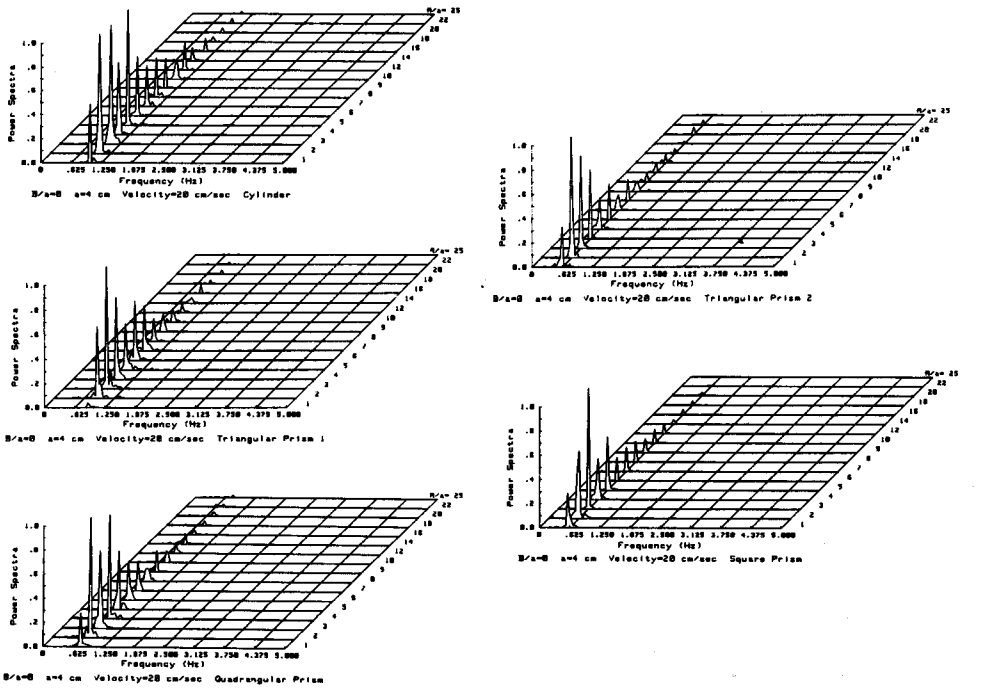

Fig. 13. Comparison of power spectra in back eddy area.

ized by strong fluctuations and the second by gentler ones.

Because the frequency was a constant in the eddy area, the unchangeable frequency can be used to define the effective eddy area, i.e., in the effective eddy area, the dominant frequency of the eddy generated by an object remains unchanged and the energy concentrated at the dominant frequency is higher than the energy of the noise level. Based on this definition it was found that the cylinder had the most distant effective eddy area, which was greater than $A/a=25$, in contrast to the square prism, which had the shortest effective eddy area of approximately $A/a=23$.

Expansion of the eddy area was also examined and it was found that the expansion and strength of the eddy were different for each model in terms of the maximum pressure in analog data (Fig. 14). It is apparent that the eddy generated by the square prism had the widest eddy area and the strongest eddy strength; the eddy generated by the cylinder had the narrowest area and was the weakest. The point at which the peak value appeared was not at the central line but along the sides. When comparing the models, it was found that the peak point shifted toward the side from $B/a=0.85$ to $B/a=1.85$ and the eddy strength changed from $CP_x=1.88$ to $CP_x=3.34$. Based on the analog data obtained along the central line ($B/a=0$) and the cross line ($A/a=5$), the maximum eddy strength for each model in the eddy area was calculated through the rates of the peak value in the central line to the peak value in the cross line (Table 4). The peak points were modified, assuming that the parameters were continuous variables.

Further, the power spectra of different models along the cross line were analyzed (Fig. 15). It was found that the dominant frequency was also a constant in the two side eddy areas. Using the definition of the effective eddy area, it was found that the cylinder had the most narrow effective eddy range, which was approximately $B/a=2.5$, and the square prism had the widest effective range, which was wider than $B/a=4.0$.

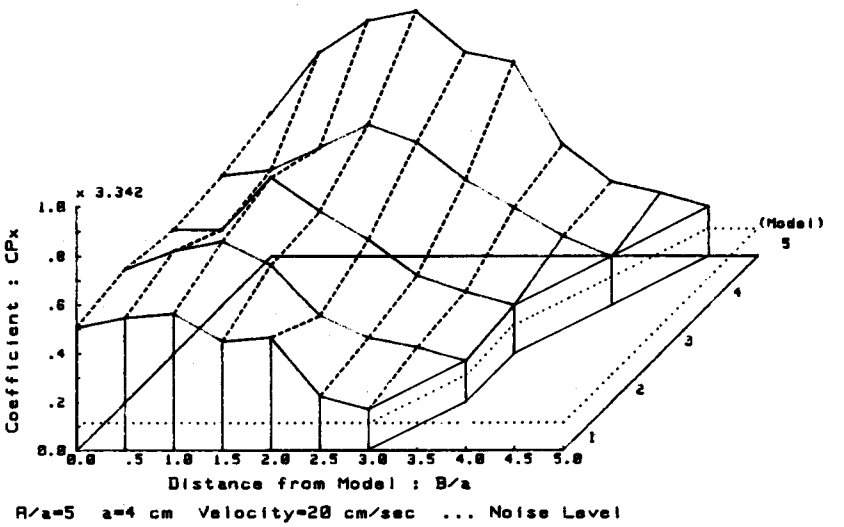

Fig. 14. Changes of pressure coefficient in side eddy area.

Table 4. Peak points and peak values of eddy strength with different models

	Cylinder	Triangular Prism 1	Quadrangular Prism	Triangular Prism 2	Square Prism
			A/a		
Peak Point B/a=0	4.00	3.45	3.00	2.25	2.00
Peak Value CPx	2.26	2.07	2.07	2.39	2.70
			B/a		
Peak Point A/a=5	0.85	1.10	1.28	1.75	1.85
Peak Value	1.88	2.20	2.39	2.45	3.34
A/a=5 B/a=0 Point Value	1.69	1.69	1.69	1.75	1.94
Maximum Peak Value	2.52	2.70	2.93	3.35	4.64

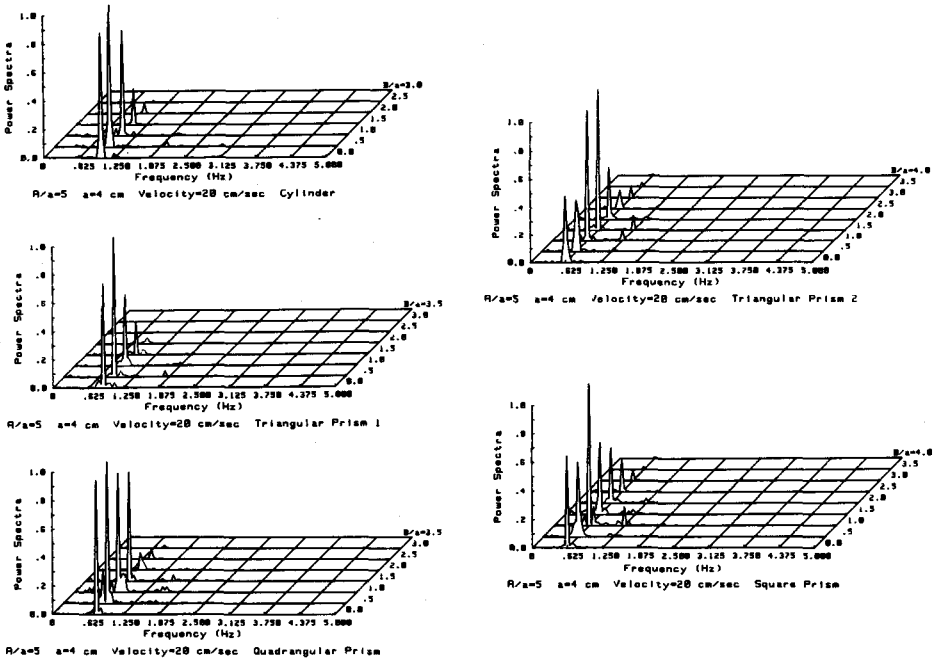

Fig. 15. Comparison of power spectra in side eddy area.

From the power spectra, another important phenomenon was discovered - in the side eddy areas there existed a subdominant frequency, the value of which was exactly twice as high as the dominant frequency.

Discussion

With the above results, it is possible to obtain a clear image about the vortices generated by representative models. In general, when an object is placed in a steady flow, an new area of influence appears around the object; the area effected by the object has distingushably different hydrodynamic characteristics from those of the previously uninterrupted flow area. With a certain unchangeable parameter, i. e., the frequency of the eddy generated by the object, the influence area exists in the flow field.

Experimental results indicate that the area of influence has different forms in terms of physical stimuli, i.e., frequency, strength, and effective influence range of the eddy, which vary with different models. Comparing the hydrodynamic characteristics in influence areas effected by different models, it was found that the higher the frequency of the eddy, the weaker its variation in strength and, conversely, the greater its variation in strength, the lower its frequency. If this phenomenon is analyzed in terms of energy, it is obvious that energy is conserved when the eddy is generated by an object, since the energy of the eddy can be formulated as: $E \propto W^2 \cdot f^2$, where W expresses the strength of the eddy and f is the dominant frequency of the eddy. However, the shape of the model plays an important role in transforming the original energy from the uniform flow into an eddy. When the effective eddy area is analyzed, it is observed that a greater width accompanies a shorter distance and, conversely, a narrower width has a greater distance; all of these changes being interrelated with the strength and frequency of the eddy.

Comparing similar models of different sizes, it was found that the influence areas are geometrically similar and at geometrically similar points, the eddy strength has the same value. This phenomenon can be explained by the fact that the increased energy of the eddy caused by the increased size changes the influence area but does not change the eddy strength. Using the formula: $F \propto SU^2$, where F is the drag of the model and S is the projected area of the model, $F_1/F_2 = S_1/S_2 = a_1/a_2 = A_1/A_2$ is obtained for similar models of different sizes. With this formula, changes in the energy of the eddy generated by the similar models can be easily understood.

In the effective eddy area, properties of physical excitations are the same in terms of frequency, i.e., the energy is concentrated at one frequency. In this frequency, the pressure is transmitted to the side areas and as a result, a physical excitation field is established around an object. Considering the distribution of the eddy strength and energy attenuation, the effective eddy area can be defined as two distinct phenomena: strong change, i.e., a stronger excitation field exists; and, weak change, i.e., a weaker excitation field exists. The range changes conversely in terms of width and distance.

Among those parameters relating to eddies, only one type of object can be utilized for getting one maximum value of physical variation from them. Variations of those parameters obey the law of Conservation of Energy. In designing the optimal artificial reef, this law is extremely important for engineering research in this field. If the stronger pressure to effect organisms is desirable, then a structure that generates an eddy with a lower frequency should be designed. To creat a

higher frequency to lure organisms, a structure that generates an eddy with a weaker pressure should be designed. The eddy range should also be considered along with size, scale and design of artificial reef structure. If the structures are carefully designed, a frequency that is more effective at attracting a target species can be obtained and the optimal artificial reefs, which have specific functions, can also be designed.

To date, random dumping of the units onto the seabed has been the usual placing method. Thus, the randomly dumped units have formed very diverse and irregular artificial reef structures. In the sea, the water movement caused by tides and currents will generate distinguishably different physical stimuli around the artificial reefs, such as eddy strength, frequency of vortices and effective range of the eddy. However, because the structures are all different in size and shape and their placement and design are uncontrolled, the effects on the environment are unknown. It is well known that any organism has an optimal range for adapting to environmental conditions. In the vicinity of artificial reefs there exists an area of influence where physical excitations are generated by the reefs themselves. Comparing patterns of strength distribution, if an artificial reef structure, which is randomly placed, generates an excitation field to which the organisms could hardly adapt, then the placement of the artificial reef becomes totally ineffectual. Generally, various organisms will gather in the vicinity of artificial reefs because the physical stimuli are attenuated and vary extensively in range.

Analysing the artificial reef structure from a hydrodynamic point of view, several suggestions for optimum use can be made as follows: 1) In order to design an effective structure, the different shapes of components as basic design elements should be considered. 2) For a high frequency to lure fish, components of a narrower width should be utilized. 3) To increase pressure for effecting fish, prism, not cylinder, should be utilized as the basic design elements. 4) To increase the size of the influence area, larger sized components should be incorporated into the design of artificial reef structures.

Acknowledgements

The authors wish to express sincere thanks to Dr. Katsuaki Nashimoto, Dr. Katsutaro Yamamoto and Prof. Shuzo Igarashi, Faculty of Fisheries, Hokkaido University, for their valuable advice and useful discussions and also to the graduated students who have given their assistance during this study.

References

Adachi, T. and R. Matsumoto. (1981). Similar distribution of the disturbance wake behind an object. *Trans. Jap. Soc. Mechanical Engineers. Series B*, **47** (422), 1933-1939. (In Japanese).

Artificial Reef Comprehensive Research Association (in Japan). (1976). A Review of Artificial Fishreef Research—I: Primary subjects of artificial fishreef study. *Suisan Zoyoshoku Sosho* **26**, 9-39. (In Japanese).

Asanuma, T. (1979). *Flow Visualization Handbook*. 377 p. Ihshisaki bookstore, Tokyo. (In Japanese).

Bohnsack, J.A. and D.J. Sutherland. (1985). Artificial Reef Research: A Review with Recom-

mendations for Future Priorities. *Bull. Amer. Mar. Sci.* **37** (1), 11-39.

Burchmore, J.J., D.A. Pollard, J.D. Bell, M.J. Middleton, B.C. Pease and J. Matthews. (1985). An ecological comparison of artificial and natural rocky reef fish communities in Botany Bay, New South Wales, Australia. *Bull. Amer. Mar. Sci.* **37** (1), 70-85.

Chang, L. (1985). Review of artificial reefs in Taiwan : Emphasizing site selection and effectiveness. *Bull. Amer. Mar. Sci.* **37** (1), 143-150.

D'Itri, F.M. (1985). *ARTIFICIAL REEFS, Marine and Freshwater Applications.* 589 p. Lewis Publishers Inc., Michigan.

Feigenbaum, D., H.B. Carvel, M. Bell, J.R. Martin and M.G. Kelly. (1985). Virginia's artificial reef study, description and results of year I. *Bull. Amer. Mar. Sci.* **37** (1), 179-188.

Hino, M. (1977). *Spectral Analysis.* 300 p. Asakura Bookstore, Tokyo. (In Japnese).

Hori, Y. (1985). Artificial reefs in Ihbaraki Prefecture. Bull. Jap. Soc. *Fisheries Oceanography.* **47-48**, 147-150. (In Japanese).

Igarashi, T. (1984). Characteristics of the flow around square prisms. *Transactions of the Japan Society of Mechanical Engineers. Series B,* **50** (449), 210-217. (In Japanese).

Jessee, W.N., A.L. Carpenter and J.W. Carter. (1985). Distribution patterns and density estimates of fishes on a southern California artificial reef with comparisons to natural Kelp-Reef habitats. *Bull. Amer. Mar. Sci.* **37** (1), 214-226.

Kanamoto, G. (1959). *Hydraulics-2.* 398 p. Kyouritsu Publishers Inc., Tokyo. (In Japanese).

Matthews, K.R. (1985). Species similarity and movement of fishes on natural and artificial reefs in Monterey Bay, California. *Bull. Amer. Mar. Sci.* **37** (1), 252-270.

Nakahara, D. (1982). Distribution patterns of artificial reef units and productivity. *Fishes and Reefs.* **3** (3), 4-9. (In Japanese).

Nakamura, M. (1985). Evolution of artificial fishing reef concepts in Japan. *Bull. Amer. Mar. Sci.* **37** (1), 271-278.

Noto, K., J. Yoshida and R. Matsumoto. (1983). Visualization of breakdown of the Karman Vortex street due to natural convection. *Flow visualization. Jap.* **3** (10), 127-132. (In Japanese With English abstract).

Ogawa, Y. (1967). Experiments on the attractiveness of artificial reefs for marine fishes. VII. Attraction of fishes to the various sizes of model reefs. *Bull. Jap. Soc. Fish.* **33**, 801-811. (In Japanese).

Ohshima, Y. (1954). *Housing scheme for fishes.* 56 p. Ihshisaki Bookstore, Tokyo. (In Japanese).

Pollard, D.A. and J. Matthews. (1985). Experience in the construction and siting of artificial reefs and fish aggregation devices in Australian waters, with notes on and a bibliography of Australian studies. *Bull. Amer. Mar. Sci.* **37** (1), 299-304.

Resource Association of Japan. (1983). *Cultivating Fishery.* 752 p. the Statistics Aassociation of Aagriculture, Forestry and Fisheries, Tokyo. (In Japanese).

Sakuda, H., M. Sakuda, K. Wadanabe and H. Ohnishi. (1982). Flow visualization around artificial reef model. *Flow Visualization.* **2**, Suppl., 29-32. (In Japanese with English abstract).

Sato, O. (1977). Several problems about artificial reefs. *Coastal Oceanography Study Note.* **14**, 88-100. (In Japanese).

Sato, O. (1984). *Artificial Reefs. The Series of Fisheries 51.* 130 p. Kousei Publishers Inc., Tokyo. (In Japanese).

Sonu, C.J. (1981). *Review of Japanese Fishing Reef Technology. Sierra Madre, Tekmarine project TCN-017, Final Report, 3-21.*

Stone, R.B. (1985). History of artificial reef use in the United States. Pages 3-11 in F.M. D'Itri, ed. Artificial Reefs, marine and freshwater applications. Lowis Publishers Inc., Michigan.

Takahashi, H. (1973). Fast Fourier Transform (FFT). *Information Processing. Jap.* **14** (8), 571-574. (In Japanese).

Yamane, H. (1984). Establishment of fishing ground and a prospect for the future. *Fishery Cooperation Association. Jap.* **2**, 16-25. (In Japanese).

Yonezawa, Y. and K. Takasuka. (1972). Optimal numbers of data for FFT algorithm to decrease calculation time. *Information Processing.* **13** (6), 571-574. (In Japanese).

Yoshizawa, M. (1969). What's the FFT ?—a new algorithm about Fourier Transform. *Diamond Mathematical Science. Jan.* **7** (6), 42-50. (In Japanese).